Cell Calcium 79 (2019) 68–74

Contents lists available at ScienceDirect

Cell Calcium

journal homepage: www.elsevier.com/locate/ceca

L-type calcium channel modulates mechanosensitivity of the cardiomyocyte cell line H9c2

Ken Takahashi[a,b,*], Shogo Hayashi[b], Mari Miyajima[b], Marei Omori[b], Jing Wang[a,c], Keiko Kaihara[a], Masatoshi Morimatsu[a], Chen Wang[a], Jian Chen[a,d], Gentaro Iribe[a], Keiji Naruse[a], Masahiro Sokabe[b,e]

[a] Department of Cardiovascular Physiology, Graduate School of Medicine, Dentistry and Pharmaceutical Sciences, Okayama University, Okayama, Japan
[b] Department of Physiology, Nagoya University School of Medicine, Nagoya, 466-8550, Japan
[c] Department of Cardiology, Qingdao Municipal Hospital, Qingdao, 266001, China
[d] Department of Pathophysiology, School of Basic Medical Sciences, Harbin Medical University, Harbin, 150081, China
[e] Mechanobiology Laboratory, Nagoya University Graduate School of Medicine, Nagoya, 466-8550, Japan

ARTICLE INFO

Keywords:
Voltage-gated calcium channel
Cardiomyocyte
Mechanosensitivity
Calcium-induced calcium release

ABSTRACT

The application of mechanical stimuli to cells often induce increases in intracellular calcium, affecting the regulation of a variety of cell functions. Although the mechanism of mechanotransduction-induced calcium increases has not been fully resolved, the involvement of mechanosensitive ion channels in the plasma membrane and the endoplasmic reticulum has been reported. Here, we demonstrate that voltage-gated L-type calcium channels play a critical role in the mechanosensitive calcium response in H9c2 rat cardiomyocytes. The intracellular calcium level in H9c2 cells increased in a reproducible dose-dependent manner in response to uniaxial stretching. The stretch-activated calcium response (SICR) completely disappeared in calcium-free medium, whereas thapsigargin and cyclopiazonic acid, inhibitors of sarcoendoplasmic reticulum calcium ATPase, partially reduced the SICR. These findings suggest that both calcium influx across the cell membrane and calcium release from the sarcoendoplasmic reticulum are involved in the SICR. Nifedipine, diltiazem, and verapamil, inhibitors of L-type calcium channels, reduced the SICR in a dose-dependent manner. Furthermore, small interfering RNA against the L-type calcium channel α1c subunit diminished the SICR dramatically. Nifedipine also diminished the mechanosensitivity of Langendorff-perfused rat heart. These results suggest that the SICR in H9c2 cardiomyocytes involves the activation of L-type calcium channels and subsequent calcium release from the sarcoendoplasmic reticulum.

1. Introduction

Mechanical forces play critical roles in both health and disease. Appropriate mechanical loading helps maintain the integrity and homeostasis of a variety of organs and tissues. In addition, mechanical stresses determine fate during organ development and cellular differentiation [1]. Hypertension causes pathologic enlargement of the heart [2]. These mechanical stresses elicit various biochemical responses in cells, including increases in the intracellular calcium level. For example, bone formation [3] and muscle development [4] are modulated by mechanosensitive calcium signaling. Hypertension exerts mechanical pressure on the heart chambers and mechanical stretching of cardiomyocytes, which in turn elicits calcium signaling that leads to cardiac hypertrophy [5].

The mechanosensitivity of the heart involves multiple mechanisms and types of biological machinery, including the large sarcomeric protein titin [6], cytoskeletal systems [7], and mechanosensitive ion channels [5]. The intracellular calcium ion concentration in cardiomyocytes is tightly coupled with contraction of the heart. Evidence indicates that cardiomyocytes show calcium transients in response to mechanical stimuli such as stretching, in which voltage-gated calcium channels are potential mechanotransducers [8–14]. The aim of this study was to explore the possible involvement of L-type voltage-gated calcium channels in the mechano-responses of the heart. Here, we

Abbreviations: SICR, stretch-activated calcium response

* Corresponding author at: Department of Cardiovascular Physiology, Graduate School of Medicine, Dentistry and Pharmaceutical Sciences, Okayama University, 2-5-1 Shikata-Cho, Kita-Ku, Okayama, 700-8558, Japan.
E-mail address: takah-k2@okayama-u.ac.jp (K. Takahashi).

https://doi.org/10.1016/j.ceca.2019.02.008
Received 16 July 2018; Received in revised form 1 February 2019; Accepted 18 February 2019
Available online 22 February 2019

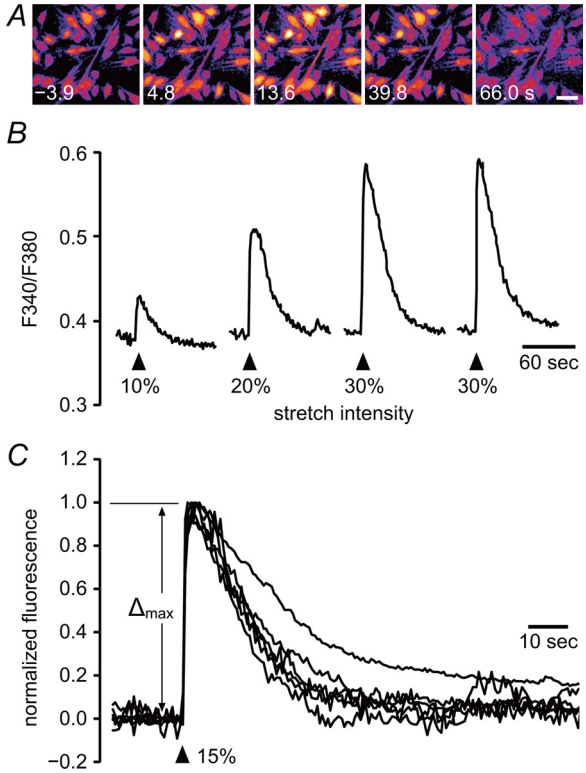

Fig. 1. Stretch stimulus induces elevation of intracellular calcium level in rat H9c2 cardiomyocytes.
A, Representative images of intracellular calcium levels using Fura-2 as a calcium indicator. Numbers at bottom left indicate seconds after 0.5-s transient stimulation of 20% stretch. Brighter pixels indicate higher calcium levels. Bar at bottom right indicates 50 μm. *B*, Stretch-induced calcium response (SICR) to sequential stretches. *C*, Representative traces of intracellular calcium responses to 15% stretch stimulus, where data were obtained from six individual cell cultures. The Δ_{max} value is defined as the peak calcium level minus the baseline level for each SICR.

report that H9c2 rat cardiomyocytes exhibit a calcium response to stretching stimuli, and this response was largely inhibited by pharmacologic blockers and silencing of the gene encoding the cardiac L-type calcium channel. Furthermore, we observed that the mechanosensitivity of Langendorff-perfused rat heart was diminished by blockade of L-type calcium channels, suggesting that these channels play a crucial role in the mechano-response of the heart *in vivo*.

2. Results

2.1. SICR in H9c2 cardiomyocytes

Intracellular calcium levels in H9c2 cardiomyocytes increased immediately after the onset of stretching stimulation and peaked 3–15 s later (Fig. 1A, B). The peak intracellular calcium value depended on stretching intensity, which was consistent within the same sample (Fig. 1B). The calcium level returned to baseline 60–120 s after the onset of stretching, and the time course of the SICR was similar between samples (Fig. 1C).

The SICR disappeared in calcium-free medium (Fig. 2A). Thapsigargin [15] and cyclopiazonic acid, inhibitors of sarcoendoplasmic reticulum calcium ATPase, were used to examine the role of calcium release from the sarcoplasmic reticulum in the SICR. At a concentration of 5 μM, thapsigargin inhibited the calcium response induced by 30% stretching by 34% ($p < 0.05$, Fig. 2A). Moreover, 100 μM cyclopiazonic acid reduced the SICR by 49% ($p < 0.001$, Fig. 2B). However, 10 μM xestospongin C (an inhibitor of inositol-1,4,5-trisphosphate [IP_3] receptor) did not affect the SICR (Fig. 2B). The trivalent lanthanide gadolinium is often used to block mechanosensitive ion channels; accordingly, we found that 10 μM Gd^{3+} almost completely blocked the SICR ($p < 0.001$, Fig. 2B). The involvement of ryanodine receptors in the SICR has also been studied. A high concentration (high micromolar range) of ryanodine was shown to abolish calcium sparks via ryanodine receptors [16,17]. However, the application of 100 μM ryanodine did not affect the SICR (data not shown).

To further characterize the SICR of H9c2 cardiomyocytes, blockers of transient receptor membrane potential (TRP) channels were applied. TRPC [18,19] and TRPV2 [20] channels are mechanosensitive. We used SKF-96365, 2-APB, and BTP2 [21,22] as TRPC blockers. Ruthenium red was used to block the TRPV2 channel. We found that 50 μM SKF-96365 inhibited the SICR by approximately 50% (Fig. 3A). Moreover, 2-APB inhibited the SICR in a dose-dependent manner (Fig. 3B). In contrast, BTP2 did not affect the response even at a concentration of 100 μM (Fig. 3A). Furthermore, 50 μM ruthenium red inhibited the SICR by approximately 70% (Fig. 3A). However, as ruthenium red is known to inhibit other types of ion channels, including Piezo channels [23], this result does not necessarily indicate that TRPV2 is involved in the SICR. Thus, we silenced the TRPV2 channel gene to confirm its involvement in the SICR. Unexpectedly, gene silencing did not significantly affect the response (Fig. 4A, B), indicating that TRPV2 has little or no impact on the SICR. Silencing of the TRPV2 gene was confirmed using quantitative RT-PCR (> 90% knockdown vs. siNEG; $p < 0.001$) (Fig. 4C).

2.2. L-type calcium channels modulate the SICR in H9c2 cardiomyocytes

L-type calcium channels play a pivotal role in regulating intracellular calcium levels in cardiomyocytes. To investigate the involvement of these channels in the SICR, we used three specific blockers: nifedipine, diltiazem, and verapamil. Each drug inhibited the SICR in a dose-dependent manner (Fig. 5A). To further examine the hypothesis that L-type calcium channels are involved in the SICR, expression of the α1c subunit of the channel was suppressed using transfected siRNA. The α1c subunit is highly expressed in cardiac muscle [24] and forms the calcium-permeating pore of the L-type calcium channel molecule [25]. Although the SICR of H9c2 cells transfected with siNEG was similar to that of untransfected control cells, that of siα1c was significantly inhibited (vs. siNEG, $p < 0.05$; vs. untransfected control, $p < 0.05$) (Fig. 5B, C). Silencing of α1c mRNA was confirmed using qRT-PCR (approximately 70% knockdown; vs. siNEG, $p < 0.001$) (Fig. 5D).

2.3. Effect of L-type calcium channel blockers on the Frank–Starling gain in rat heart

Langendorff-perfused rat hearts were used to investigate the role of L-type calcium channels in mechanosensitivity of the heart. When the volume of the left ventricle was increased using an intraventricular balloon, systolic pressure measured by a manometer connected to the balloon increased accordingly (Fig. 6A, C). The increase in the volume of the ventricle induced by the intraventricular balloon was confirmed using echocardiography (Fig. 6B). However, the mechanosensitive effect diminished upon perfusion with 0.1 μM nifedipine. After removing nifedipine from the perfusate, recovery from the pressure-induced increase in heart contractility occurred (Fig. 6A, D). We expanded the Frank–Starling gain (FSG), originally developed as an indicator of the mechanosensitivity of cardiomyocytes [26], to the *ex vivo* heart. FSG is defined as the ratio of the systolic slope to the diastolic slope. An FSG value of 1.0 indicates no increase in contraction with an increase in volume. The FSG value of 2.75 ± 0.47 decreased to 1.40 ± 0.13 in response to treatment with 0.1 μM nifedipine. The value returned to 2.42 ± 0.34 after nifedipine was removed from the perfusate (Fig. 6D). The application of nifedipine did not affect diastolic pressure (Fig. 6E).

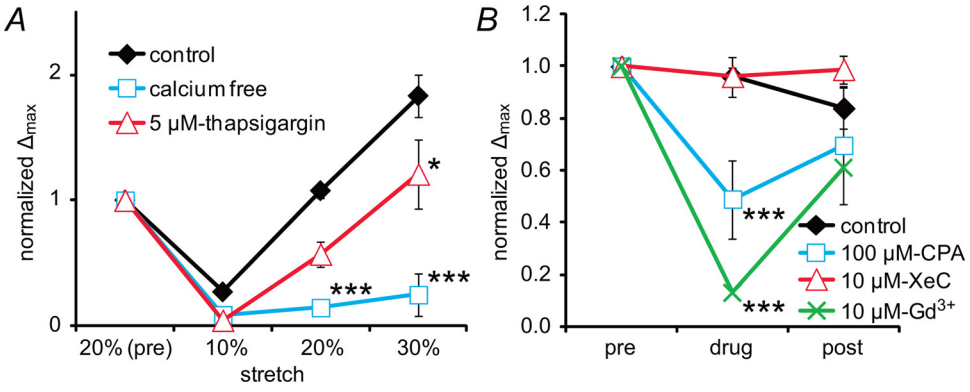

Fig. 2. Effects of potential modulators of SICR. *A*, Ca^{2+} sources in the SICR. After the bath solution was replaced, three sequential stretch stimuli (10%, 20%, and 30%) were applied. Calcium responses were normalized to the pre-treatment value. *B*, Characterization of the SICR. Stretch intensity of 15% was used for pre-, peri-, and post-treatment of chemicals. Triangles indicate the application of 15% stretch. Bars indicate SEM. Two-way repeated measures ANOVA with Bonferroni post-test was used for statistical analysis. *: $p < 0.05$, ***: $p < 0.001$ vs. control.

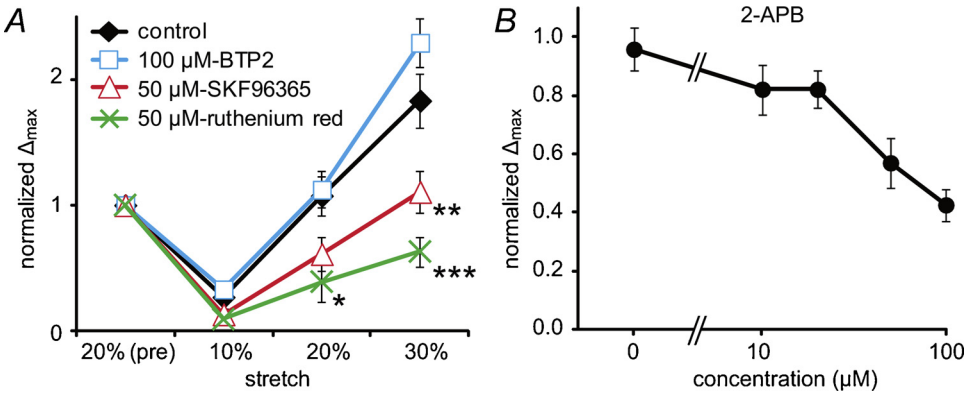

Fig. 3. Effects of TRP channel blockers on the SICR.
A, Effects of TRPV and TRPC blockers on the SICR. For each experiment, a 20% stretch was applied to obtain the pre-treatment response. After the bath solution was exchanged, three sequential stretch stimuli (10%, 20%, and 30%) were applied. Calcium responses were normalized to the pre-treatment value. *B*, Effect of the TRPC blocker 2-APB on the SICR. Bars indicate SEM. Two-way repeated measures ANOVA with Bonferroni post-test was used for statistical analysis. *: $p < 0.05$, **: $p < 0.01$, ***: $p < 0.001$ vs. control.

3. Discussion

In the current study, transient stretching caused reproducible calcium responses in H9c2 cardiomyocytes. Similar responses to mechanical stimulation were previously observed in neonatal [9] and adult cardiomyocytes [8]. A recent report also described SICR in cardiomyocytes differentiated from induced pluripotent stem cells [27]. These findings suggest that our results are not limited to the specific cell line used. Our observation that the SICR completely disappeared in calcium-free medium indicates that extracellular calcium is absolutely required for the SICR in H9c2 cells. Moreover, it has been suggested that the SICR also involves calcium release from internal calcium stores, as the SERCA inhibitors thapsigargin and cyclopiazonic acid significantly reduced the SICR. However, the SICR was not inhibited by sufficient concentrations of xestospongin C (an inhibitor of the IP_3 receptor) or ryanodine (an inhibitor of the ryanodine receptor), suggesting that these receptors are not involved in the SICR.

It is natural to hypothesize that ion channels are involved in the SICR, as the intracellular calcium level increased sharply immediately after the onset of stretching and the response required extracellular calcium. In this study, we used inhibitors of TRPC, TRPV, and L-type calcium channels to test this hypothesis. Although the TRPC inhibitors SKF-96365 and 2-APB significantly suppressed the SICR, another inhibitor, BTP2, did not. A possible explanation for these conflicting results is the low specificity of these inhibitors [28,29]. However, to clarify this issue, the use of a more direct method, such as gene knockdown, might be necessary. The TRPV inhibitor ruthenium red, which is known to exert a variety of effects on other targets, also inhibited the SICR in this study. However, it is unlikely that TRPV2 channels are involved in this phenomenon, as silencing of the TRPV2 channel gene did not significantly affect the SICR.

We tested the hypothesis that L-type calcium channels are involved in the SICR in H9c2 cardiomyocytes. This hypothesis was supported by results demonstrating that specific inhibitors of these channels (nifedipine, diltiazem, and verapamil) inhibited the SICR in a dose-dependent manner. The results of silencing the L-type calcium channel gene using siRNA further support this hypothesis. In contrast, Gd^{3+} inhibited the SICR in this study. While Gd^{3+} is commonly used to block mechanosensitive ion channels, it also inhibits the activity of L-type calcium channels [30,31]. According to Lacampagne et al., the ion current via the L-type calcium channel is completely blocked by 10 μM Gd^{3+}, the concentration that we used in this study. Although several groups have reported the mechanosensitivity of voltage-dependent L-type calcium channels [8,32–34], the results of the current research do not enable the drawing of definitive conclusions regarding this phenomenon, as it is possible that another type of mechanosensitive channel activates L-type calcium channels and induces the SICR. The mechanosensitivity of the L-type calcium channel itself in the context of cardiomyocyte mechanotransduction should be clarified in future work.

3.1. Possible involvement of L-type calcium channels in the mechanosensitivity of the beating heart

The FSG, an indicator of cardiac mechanosensitivity, decreased in response to the application of nifedipine. This suggests the involvement of L-type calcium channels in the mechanosensitivity of the beating heart. However, care should be taken when considering this effect, because the decrease in the intracellular calcium level caused by nifedipine would be expected to diminish cardiac contractility. To discriminate the possible mechanosensitive effect from the direct effect on decreasing cardiac contractility of L-type calcium channels, the intracellular calcium level should be reduced using a method other than the application of nifedipine.

The present study demonstrated not only the involvement of L-type calcium channels in the SICR of H9c2 cardiomyocytes but also the possible contribution of these channels to FSG in living rat heart. In addition to L-type calcium channels, T-type calcium channels exhibit voltage dependence. It was recently reported that T-type calcium channels are involved in the mechanosensitivity of chondrocytes [35]. Further studies are expected to elucidate the crucial roles played by

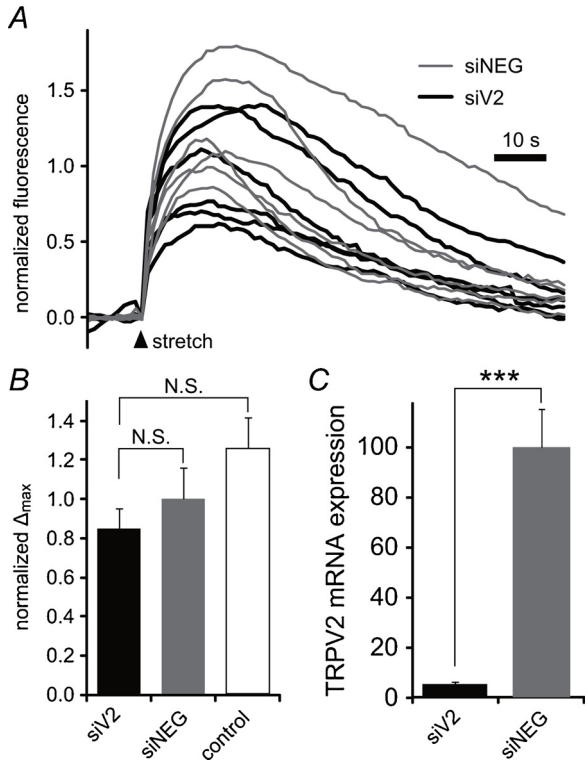

Fig. 4. Nonsignificant modulation of the SICR by TRPV2.
A, SICRs in the TRPV2-knockdown and negative control groups. Each trace represents data obtained from an individual cell culture. Black lines: cells transfected with TRPV2 siRNA (siV2); gray lines: cells transfected with control siRNA (siNEG). Each F340/F380 value is normalized to the mean of peak responses in the negative control group. n = 6 for each group. *B*, Analysis of the peak calcium response in *B*. One-way ANOVA with Bonferroni post-test was used for statistical analysis. *C*, Confirmation of gene silencing using qRT-PCR (n = 6 for each group). RNA samples were obtained from the same cells used in *A*. Rat β-actin was used as an endogenous control. The TRPV2 mRNA expression level was normalized to that of the negative control. Unpaired *t*-test was used for statistical analysis. N.S.: not significant; ***: $p < 0.001$ vs. control.

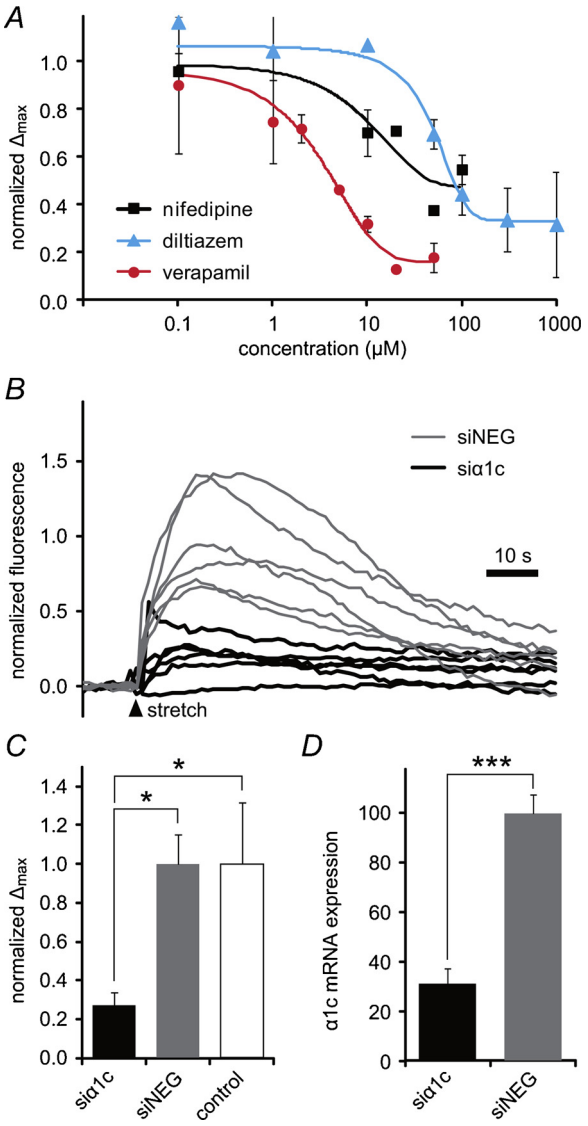

Fig. 5. L-type calcium channel modulates the SICR.
A, Dose-dependent inhibition of the SICR by nifedipine, diltiazem, and verapamil. Responses to 15% stretch were recorded and normalized to the response before drug application. *B*, Inhibition of the SICR by silencing of the gene encoding the α1c subunit of the L-type calcium channel. Each trace represents data obtained from an individual cell culture. Black lines: cells transfected with α1c siRNA (siα1c); gray lines: cells transfected with control siRNA (siNEG). Each F340/F380 value was normalized to the mean of peak responses in the negative control group. n = 6 for each group. *C*, Analysis of the peak calcium response in *B*. One-way ANOVA with Bonferroni post-test was used for statistical analysis. *D*, Confirmation of gene silencing using qRT-PCR (n = 6 for each group). RNA samples were obtained from the same cells used in *B*. Rat β-actin was used as an endogenous control. α1c mRNA expression level was normalized to that of the negative control. Unpaired *t*-test was used for statistical analysis. *: $p < 0.05$, ***: $p < 0.001$ vs. control.

voltage-gated calcium channels in the mechanosensitive responses of a variety of cells other than cardiomyocytes.

4. Methods

4.1. Cell culture

H9c2 cells were obtained from the American Type Culture Collection (ATCC, Manassas, VA, USA). The cells were cultured in Dulbecco's Modified Eagle's Medium containing 10% fetal calf serum and used within 10 passages. Elastic silicone chambers with bottom dimensions of 2 × 2 cm were used. The chambers were pretreated with 200 μL of 50 μM fibronectin solution in 37 °C for 1 h. H9c2 cells were plated on the chamber and cultured for 2 to 3 days and used for experiments at approximately 80% confluence. All experiments were performed with at least five different dispersions of cells from different culture dishes.

4.2. Solutions

Standard extracellular solution (SES) was prepared as follows: 140 mM NaCl; 5 mM KCl; 2 mM $CaCl_2$; 10 mM glucose; and 10 mM HEPES, with pH adjusted to 7.4 with NaOH. SKF-96365 and BTP2 were purchased from Calbiochem (Merck Millipore, Tokyo, Japan). Ryanodine was purchased from Sigma (Sigma-Aldrich Japan, Tokyo, Japan). Thapsigargin, nifedipine, diltiazem, and verapamil were purchased from Wako (Wako Pure Chemical Industries, Ltd., Osaka, Japan). Nifedipine and verapamil were dissolved in DMSO and ethanol, respectively, and diluted with SES to a final solvent concentration of less than 0.1%.

4.3. Calcium imaging

Cells were loaded with 5 μM Fura2-AM (Life Technologies, CA, USA) in a 37 °C incubator for 60 min. After incubation, the Fura2 solution was replaced with SES and the cells were kept at room temperature for

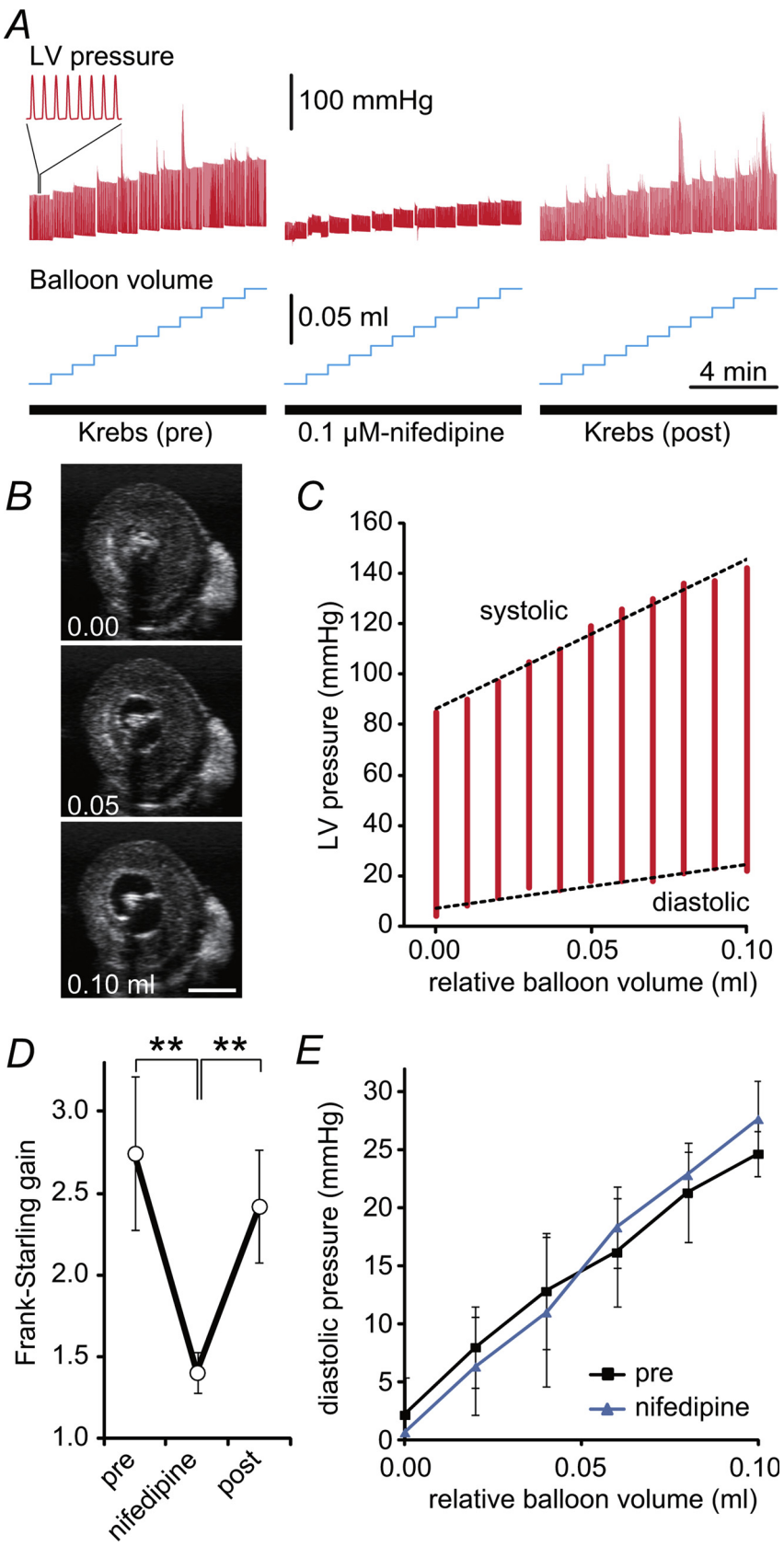

Fig. 6. Pressure–volume relationship of the heart is affected by the L-type calcium channel blocker nifedipine.
A, Recording of left ventricular pressure in Langendorff-perfused rat heart. Stair-like curves at the bottom indicate volume loading to the left ventricle. For pressure values, the balloon pressure at the same volume in air was subtracted. *B*, Cross-sectional echocardiographic images of a Langendorff-perfused heart. Numbers at bottom left indicate volume of the balloon inserted into the left ventricle. The black circular area in the center indicates the balloon filled with water. The white bar at bottom right indicates 5 mm. *C*, Pressure–volume (PV) relationship of the left ventricle obtained from *A*. In the Langendorff configuration, a circular PV-loop seen *in vivo* assumes a linear form because the balloon volume is fixed. Contraction was in a steady state at each volume during the period of PV analysis. *D*, Frank–Starling gain (FSG) obtained from *C* (n = 6). One-way repeated measures ANOVA with Bonferroni post-test was used for statistical analysis. *E*, Comparison of diastolic pressure before and during nifedipine application. **: $p < 0.01$.

20 min. An Aquacosmos system (Hamamatsu Photonics, Hamamatsu, Japan) was used to measure intracellular calcium levels. To apply uniaxial stretching to cells, the silicone chamber was stretched using a computer-controlled stretch system (STREX, Osaka, Japan) [36]. The duration of all stretch stimuli used in this experiment was 0.5 s. When the effects of chemicals were analyzed, stretch stimulus was applied at least 10 min after the application of the chemicals. An interval of at least 5 min was given between consecutive stretch stimuli. For analysis

of the intracellular calcium level, pixels that had an F340/F380 ratio of > 0.1 (overlapping with the area of cells) were chosen from the whole image containing several tens of cells, and then the F340/F380 ratio was averaged. The Δ_{max} value, defined as the peak calcium level minus the baseline level, was used as an indicator of the intensity of the SICR for each stimulus. In the text, *n* denotes the number of individual silicone chambers from different cell cultures. Experiments were carried out at room temperature (~24 °C).

4.4. RNA interference

siRNAs against the α1C subunit of the L-type calcium channel (hereafter called siα1C) and the transient receptor potential vanilloid 2 (TRPV2) (siV2), as well as negative control siRNA (siNEG), were purchased from Life Technologies. Details regarding each siRNA are as follows: siα1C, Silencer Select Pre-designed siRNA (ID: s127529); siV2, Silencer Select Pre-designed siRNA (ID: s131478); and siNEG, Silencer Negative Control #1 siRNA (ID: AM4636). Transfection of H9c2 cardiomyocytes with the siRNAs was performed using Lipofectamine RNAiMAX reagent (Life Technologies), in accordance with the manufacturer's instructions.

4.5. Quantitative reverse transcription PCR (qRT-PCR)

Transcription of the genes encoding the α1C subunit of the L-type calcium channel, $Ca_v1.2$, and the TRPV2 channel in H9c2 cardiomyocytes used in the RNAi experiments was analyzed by real-time PCR. After the calcium imaging experiments, extraction of DNA-free total RNA was carried out using an RNaqueous 4PCR RNA isolation kit (Life Technologies), in accordance with the manufacturer's instructions. Reverse transcription was carried out using a High-Capacity cDNA Reverse Transcription kit (Life Technologies) with random primers, in accordance with the manufacturer's instructions. We used the Mx3000 P qPCR System (Agilent Technologies, CA, USA) to amplify and quantify cDNAs. TaqMan assay (Life Technologies) was used in all reactions. Relative mRNA levels were calculated according to the $\Delta\Delta C_t$ method, using β-actin as an endogenous control. The TaqMan primers used were as follows: α1C, Rn00709287_m1; TRPV2, Rn00567974_m1; and rat β-actin, 4352340E.

4.6. Measurement of cardiac contractility using isolated rat hearts

Female Wistar rats aged 56–63 weeks were used. The Animal Care and Use Committee of Okayama University approved our protocol for conducting the animal experiments (permit number: OKU-2010338). All surgeries were performed under sodium pentobarbital anesthesia, and every effort was made to minimize suffering. We used a procedure described elsewhere to record the left ventricular pressure of excised rat hearts [37]. Briefly, the heart was extracted from each rat and retrogradely perfused with Krebs–Henseleit solution via the aorta. The composition of this solution was as follows: 118.5 mM NaCl; 4.7 mM KCl; 2.5 mM $CaCl_2{\cdot}2H_2O$; 1.2 mM $MgSO_4$; 11 mM glucose; and 25 mM $NaHCO_3$. The solution was bubbled with 95% O_2/5% CO_2 gas, and its temperature was maintained at 37 °C A balloon was installed into the left ventricle to record the pressure. This balloon was filled with water so that the end-diastolic pressure was less than 10 mm Hg before recording, and the relative volume of the balloon in this condition was defined as 0 ml. We used an echocardiography scanner to observe the left ventricle in which the balloon had been installed (Aplio SSA-770 A; Toshiba Medical Systems, Tochigi, Japan). The heart was not paced electrically and allowed to beat spontaneously.

4.7. Statistical analysis

All data are expressed as mean ± standard error of the mean (SEM) and analyzed using Prism software (version 5.0; GraphPad Software, La Jolla, CA, USA). For analysis of calcium responses, two-way repeated measures analysis of variance (ANOVA) was performed, followed by the Bonferroni post hoc test. For analyses of calcium responses and mRNA expression in the RNAi experiments, one-way ANOVA was performed, followed by the Bonferroni post hoc test. For analysis of FSG, one-way repeated measures ANOVA was performed, followed by the Bonferroni post hoc test. $p < 0.05$ was considered significant.

Conflict of interest

We wish to confirm that there are no known conflicts of interest associated with this publication and there has been no significant financial support for this work that could have influenced its outcome.

We confirm that the manuscript has been read and approved by all named authors and that there are no other persons who satisfied the criteria for authorship but are not listed. We further confirm that the order of authors listed in the manuscript has been approved by all of us.

We confirm that we have given due consideration to the protection of intellectual property associated with this work and that there are no impediments to publication, including the timing of publication, with respect to intellectual property. In so doing we confirm that we have followed the regulations of our institutions concerning intellectual property.

We further confirm that any aspect of the work covered in this manuscript that has involved either experimental animals or human patients has been conducted with the ethical approval of all relevant bodies and that such approvals are acknowledged within the manuscript.

We understand that the Corresponding Author is the sole contact for the Editorial process (including Editorial Manager and direct communications with the office). He is responsible for communicating with the other authors about progress, submissions of revisions and final approval of proofs. We confirm that we have provided a current, correct email address which is accessible by the Corresponding Author and which has been configured to accept email from takah-k2@okayama-u.ac.jp.

Acknowledgement

This study was supported by a Grant-in-Aid for Scientific Research on Innovative Areas [No. 15H05936].

Appendix A. Supplementary data

Supplementary material related to this article can be found, in the online version, at doi:https://doi.org/10.1016/j.ceca.2019.02.008.

References

[1] A.J. Engler, S. Sen, H.L. Sweeney, D.E. Discher, Matrix elasticity directs stem cell lineage specification, Cell 126 (2006) 677–689.
[2] K. Takahashi, H. Piao, K. Naruse, Dynamic remodeling of the heart and blood vessels: implications of health and disease, in: S.C.F. Rawlinson (Ed.), Mechanobiology: Exploitation for Medical Benefit, Wiley Blackwell, Hoboken, New Jersey, 2017, pp. 175–189.
[3] W.R. Thompson, C.T. Rubin, J. Rubin, Mechanical regulation of signaling pathways in bone, Gene 503 (2012) 179–193.
[4] T. Benavides Damm, M. Egli, Calcium's role in mechanotransduction during muscle development, Cell. Physiol. Biochem. 33 (2014) 249–272.
[5] K. Takahashi, Y. Kakimoto, K. Toda, K. Naruse, Mechanobiology in cardiac physiology and diseases, J. Cell. Mol. Med. 17 (2013) 225–232.
[6] R. Knoll, M. Hoshijima, H.M. Hoffman, V. Person, I. Lorenzen-Schmidt, M.L. Bang, T. Hayashi, N. Shiga, H. Yasukawa, W. Schaper, W. McKenna, M. Yokoyama, N.J. Schork, J.H. Omens, A.D. McCulloch, A. Kimura, C.C. Gregorio, W. Poller, J. Schaper, H.P. Schultheiss, K.R. Chien, The cardiac mechanical stretch sensor machinery involves a Z disc complex that is defective in a subset of human dilated cardiomyopathy, Cell 111 (2002) 943–955.
[7] K. Hayakawa, H. Tatsumi, M. Sokabe, Actin filaments function as a tension sensor by tension-dependent binding of cofilin to the filament, J. Cell Biol. 195 (2011) 721–727.
[8] S. Lee, J.C. Kim, Y.H. Li, M.J. Son, S.H. Woo, Fluid pressure modulates L-type Ca2+

channel via enhancement of Ca2+-induced Ca2+ release in rat ventricular myocytes, Am. J. Physiol.-Cell Physiol. 294 (2008) C966–C976.
[9] X.D. Liao, A.H. Tang, Q. Chen, H.J. Jin, C.H. Wu, L.Y. Chen, S.Q. Wang, Role of Ca2+ signaling in initiation of stretch-induced apoptosis in neonatal heart cells, Biochem. Biophys. Res. Commun. 310 (2003) 405–411.
[10] B.L. Prosser, C.W. Ward, W.J. Lederer, X-ROS signaling: rapid mechano-chemo transduction in heart, Science 333 (2011) 1440–1445.
[11] G. Iribe, C.W. Ward, P. Camelliti, C. Bollensdorff, F. Mason, R.A. Burton, A. Garny, M.K. Morphew, A. Hoenger, W.J. Lederer, P. Kohl, Axial stretch of rat single ventricular cardiomyocytes causes an acute and transient increase in Ca2+ spark rate, Circ. Res. 104 (2009) 787–795.
[12] M.D. Teichmann, F.V. Wegner, R.H. Fink, J.S. Chamberlain, B.S. Launikonis, B. Martinac, O. Friedrich, Inhibitory control over Ca(2+) sparks via mechanosensitive channels is disrupted in dystrophin deficient muscle but restored by mini-dystrophin expression, PLoS One 3 (2008) e3644.
[13] P. Zhang, A.S. Lader, M.A. Etcheverry, H.F. Cantiello, Crotoxin potentiates L-type calcium currents and modulates the action potential of neonatal rat cardiomyocytes, Toxicon 55 (2010) 1236–1243.
[14] W. Rottbauer, K. Baker, Z.G. Wo, M.A. Mohideen, H.F. Cantiello, M.C. Fishman, Growth and function of the embryonic heart depend upon the cardiac-specific L-type calcium channel alpha1 subunit, Dev. Cell 1 (2001) 265–275.
[15] J. Lytton, M. Westlin, M.R. Hanley, Thapsigargin inhibits the sarcoplasmic or endoplasmic reticulum Ca-ATPase family of calcium pumps, J. Biol. Chem. 266 (1991) 17067–17071.
[16] N.L. Thomas, A.J. Williams, Pharmacology of ryanodine receptors and Ca2+-induced Ca2+ release, Wiley Interdiscip. Rev. Membr. Transp. Signal. 1 (2012) 383–397.
[17] K. Kaihara, M. Morimatsu, C. Wang, J. Chen, G. Iribe, K. Takahashi, K. Naruse, TRPV2 channel expression and the effects of BTP2, xestospongin C, and ryanodine on calcium spark in rodent cardiomyocytes, Data Brief (2019) (submitting).
[18] R. Maroto, A. Raso, T.G. Wood, A. Kurosky, B. Martinac, O.P. Hamill, TRPC1 forms the stretch-activated cation channel in vertebrate cells, Nat. Cell Biol. 7 (2005) 179–185.
[19] M.A. Spassova, T. Hewavitharana, W. Xu, J. Soboloff, D.L. Gill, A common mechanism underlies stretch activation and receptor activation of TRPC6 channels, Proc. Natl. Acad. Sci. U. S. A. 103 (2006) 16586–16591.
[20] K. Muraki, Y. Iwata, Y. Katanosaka, T. Ito, S. Ohya, M. Shigekawa, Y. Imaizumi, TRPV2 is a component of osmotically sensitive cation channels in murine aortic myocytes, Circ. Res. 93 (2003) 829–838.
[21] L.P. He, T. Hewavitharana, J. Soboloff, M.A. Spassova, D.L. Gill, A functional link between store-operated and TRPC channels revealed by the 3,5-bis(trifluoromethyl) pyrazole derivative, BTP2, J. Biol. Chem. 280 (2005) 10997–11006.
[22] S. Kiyonaka, K. Kato, M. Nishida, K. Mio, T. Numaga, Y. Sawaguchi, T. Yoshida, M. Wakamori, E. Mori, T. Numata, M. Ishii, H. Takemoto, A. Ojida, K. Watanabe, A. Uemura, H. Kurose, T. Morii, T. Kobayashi, Y. Sato, C. Sato, I. Hamachi, Y. Mori, Selective and direct inhibition of TRPC3 channels underlies biological activities of a pyrazole compound, Proc. Natl. Acad. Sci. U. S. A. 106 (2009) 5400–5405.
[23] B. Coste, B. Xiao, J.S. Santos, R. Syeda, J. Grandl, K.S. Spencer, S.E. Kim, M. Schmidt, J. Mathur, A.E. Dubin, M. Montal, A. Patapoutian, Piezo proteins are pore-forming subunits of mechanically activated channels, Nature 483 (2012) 176–181.
[24] I. Bodi, G. Mikala, S.E. Koch, S.A. Akhter, A. Schwartz, The L-type calcium channel in the heart: the beat goes on, J. Clin. Invest. 115 (2005) 3306–3317.
[25] D. Singer, M. Biel, I. Lotan, V. Flockerzi, F. Hofmann, N. Dascal, The roles of the subunits in the function of the calcium channel, Science 253 (1991) 1553–1557.
[26] C. Bollensdorff, O. Lookin, P. Kohl, Assessment of contractility in intact ventricular cardiomyocytes using the dimensionless' Frank-Starling Gain' index, Pflugers Arch. 462 (2011) 39–48.
[27] J. Lu, Y.K. Lee, X. Ran, W.H. Lai, R.A. Li, W. Keung, K. Tse, H.F. Tse, X. Yao, An abnormal TRPV4-related cytosolic Ca(2+) rise in response to uniaxial stretch in induced pluripotent stem cells-derived cardiomyocytes from dilated cardiomyopathy patients, Biochim. Biophys. Acta 1863 (2017) 2964–2972.
[28] M.G. Rae, J. Hilton, J. Sharkey, Putative TRP channel antagonists, SKF 96365, flufenamic acid and 2-APB, are non-competitive antagonists at recombinant human alpha1beta2gamma2 GABA(A) receptors, Neurochem. Int. 60 (2012) 543–554.
[29] V. Juvin, A. Penna, J. Chemin, Y.L. Lin, F.A. Rassendren, Pharmacological characterization and molecular determinants of the activation of transient receptor potential V2 channel orthologs by 2-aminoethoxydiphenyl borate, Mol. Pharmacol. 72 (2007) 1258–1268.
[30] A. Lacampagne, F. Gannier, J. Argibay, D. Garnier, J.-Y. Le Guennec, The stretch-activated ion channel blocker gadolinium also blocks L-type calcium channels in isolated ventricular myocytes of the guinea-pig, Biochim. Biophys. Acta (BBA) – Biomembr. 1191 (1994) 205–208.
[31] A. Malasics, D. Boda, M. Valisko, D. Henderson, D. Gillespie, Simulations of calcium channel block by trivalent cations: Gd(3+) competes with permeant ions for the selectivity filter, Biochim. Biophys. Acta 1798 (2010) 2013–2021.
[32] G.L. Lyford, P.R. Strege, A. Shepard, Y.J. Ou, L. Ermilov, S.M. Miller, S.J. Gibbons, J.L. Rae, J.H. Szurszewski, G. Farrugia, Alpha(1C) (Ca(v)1.2) L-type calcium channel mediates mechanosensitive calcium regulation, Am. J. Physiol., Cell Physiol. 283 (2002) C1001–C1008.
[33] S.Q. Peng, R.K. Hajela, W.D. Atchison, Fluid flow-induced increase in inward Ba2+ current expressed in HEK293 cells transiently transfected with human neuronal L-type Ca2+ channels, Brain Res. 1045 (2005) 116–123.
[34] J.H. Kim, P.L. Rhee, T.M. Kang, Actin cytoskeletons regulate the stretch-induced increase of Ca2+ current in human gastric myocytes, Biochem. Biophys. Res. Commun. 352 (2007) 503–508.
[35] M. Lv, Y. Zhou, X. Chen, L. Han, L. Wang, X.L. Lu, Calcium signaling of in situ chondrocytes in articular cartilage under compressive loading: roles of calcium sources and cell membrane ion channels, J. Orthop. Res. 36 (2018) 730–738.
[36] K. Murase, K. Naruse, A. Kimura, K. Okumura, T. Hayakawa, M. Sokabe, Protamine augments stretch induced calcium increase in vascular endothelium, Br. J. Pharmacol. 134 (2001) 1403–1410.
[37] J. Wang, K. Takahashi, H. Piao, P. Qu, K. Naruse, 9-Phenanthrol, a TRPM4 inhibitor, protects isolated rat hearts from ischemia-reperfusion injury, PLoS One 8 (2013) e70587.